PHYSICAL REVIEW B VOLUME 12, NUMBER 8 15 OCTOBER 1975

Interchain coupling and the Peierls transition in linear-chain systems*

B. Horovitz and H. Gutfreund
The Racah Institute of Physics, The Hebrew University, Jerusalem, Israel

M. Weger
Nuclear Research Center, Negev, Post Office Box 9001, Beer-Sheva, Israel
and The Racah Institute of Physics, The Hebrew University, Jerusalem, Israel

(Received 6 January 1975)

We study the effect of interchain coupling on the Peierls transition temperature T_P for a model with a nonplanar Fermi surface. Using the standard electron-phonon coupling, we show that the soft mode which causes the transition should have a wave vector $q_0 = (\pi/a, \pi/a, 2p_F)$. We evaluate the effect of interchain coupling on T_P within the mean-field theory, as well as the effect of fluctuations. Both these effects reduce T_P, but we find that there is a range of interchain coupling where this reduction, due to both effects, is small. Neutron-scattering cross section and fluctuation contribution to the specific heat are evaluated. Comparison is made with experiments on $K_2Pt(CN)_4Br_{0.3}\cdot 3H_2O$ (KCP) and tetrathiofulvalene-tetracyanoquinodimethan (TTF-TCNQ).

I. INTRODUCTION

One-dimensional theories have recently gained a new interest due to extensive studies on organic conductors like the tetrathiofulvalene-tetracyanoquinodimethan (TTF-TCNQ) charge-transfer salt[1] and the Krogman compounds, such as $K_2Pt(CN)_4Br_{0.3}\cdot 3H_2O$ (KCP).[2] These materials have a linear-chain structure such that the interchain coupling is much smaller than the intrachain coupling. This is reflected in the conductivity ratio $\sigma_\parallel/\sigma_\perp$, which is of order 10^3 for TTF-TCNQ, and 10^5 for KCP at room temperature.

Also related to these systems are the intermetallic compounds of the $A15$ (β-tungsten) crystal structure.[3] These consist of three perpendicular families of chains which are largely independent, thus leading to a quasi-one-dimensional behavior along each chain.

The interest in these materials is motivated by the search for a high-temperature superconductor. In fact, the $A15$ have the highest known superconducting transition temperature T_c. This may be associated with their one-dimensional character. However, we should point out that uniaxial stress in the [100] direction, which leaves the chain structure intact, lowers T_c considerably.[4] Surface dependence of the tunneling gap[5] also suggests the necessity for cubic structure (or three families of coupled chains) to sustain a high T_c. The band calculations[3] also indicate that the properties of this system may depend on the high-symmetry cubic structure.

The usual BCS-type superconductivity is caused by attractive electron-electron interaction mediated by the electron-phonon interaction. However, such an interaction in a one-dimensional system leads to a Peierls transition[6] at a temperature T_P. This transition creates a lattice distortion with wave vector $2p_F$ and a gap in the electronic spectrum at the Fermi surface $p = \pm p_F$ below T_P.[7,8] Fröhlich[7] suggested that this distortion, which is a charge-density wave, may propagate along the crystal, and due to the presence of the gap, represent a superconducting state totally different from the BCS pairing state which was not known at that time. However, this Fröhlich mode may be pinned down by lattice commensurability or by impurities[9] and thus lead to the opposite extreme of an insulating phase.

A Peierls transition has been suggested for TTF-TCNQ[10,11] with $T_P \simeq 60\,^\circ$K and for KCP[12,13] with $T_P \simeq 100\,^\circ$K. We shall later on apply the present theory to these systems, but first, let us present few theoretical problems associated with the one-dimensional electron-phonon system.

Most of the available theories treat the Peierls-Fröhlich transition using mean-field theory,[6-8,14-19] although fluctuations in a one-dimensional system prevent altogether the occurrence of a phase transition at a finite temperature. Thus it is necessary to introduce some kind of interchain coupling which will enable the development of long-range order in the transverse direction and lead to a real phase transition. Using one-dimensional models, it has been argued[20] that $T_P \simeq \frac{1}{4} T_P^0$, where T_P^0 is the mean-field value of the Peierls transition temperature. The factor $\frac{1}{4}$ is somewhat arbitrary, and we shall show that it is actually a sensitive function of the interchain coupling.

Since the Peierls transition is a property of one-dimensional systems, a second problem is whether the transition exists altogether for a finite interchain coupling. This problem was

dealt with by Beni[18] using an electron dispersion which depends also on transverse coupling. If η is the ratio of the interchain to the intrachain transfer integrals and $\tau_P^0 = T_P^0/T_F$, Beni concludes that T_P^0 is finite if roughly $\eta \lesssim \tau_P^0$, although there may be some solution at $\eta \sim (\tau_P^0)^{1/2}$. Since we usually deal with $\tau_P^0 \ll 1$, there is a large region, $\tau_P^0 \lesssim \eta \lesssim (\tau_P^0)^{1/2}$, where the result is not clear.

The present work is a continuation of Ref. 15 which dealt with the mean-field theory of the one-dimensional electron-phonon system. In Sec. II, we present our model for the interchain coupling η. In Sec. III, we deal with the effect of interchain coupling on τ_P^0 and show that the region $\tau_P^0 \lesssim \eta \lesssim (\tau_P^0)^{1/2}$ has a very important physical significance. We show that for $\eta \gtrsim \tau_P^0$, the Peierls instability associated with the wave vector $q_1 = (0, 0, 2p_F)$ is suppressed, while for $\eta \lesssim (\tau_P^0)^{1/2}$ [see Eq. (3.4)], there still exists a Peierls instability associated with the wave vector $q_0 = (\pi/a, \pi/a, 2p_F)$. Actually, if exact three-dimensional electron-hole symmetry exists [Eq. (3.1)], the system is effectively one dimensional with respect to q_0, and T_P^0 is finite for any η, as large as we wish.

In Sec. IV, we deal with the problem of fluctuations. If the interchain energy is larger than the thermal energy $\eta \gtrsim \tau_P^0$, we expect mean-field theory to be valid. An explicit calculation to first order in fluctuation effects confirms this expectation. Thus the instability at q_0 has a range of η [Eq. (4.18)] for which one-dimensional mean-field theory is effectively valid. In Sec. V, we evaluate the neutron scattering cross section and compare with experiments on KCP. Later on, we evaluate the free energy and the specific heat due to fluctuations and compare with experiments on TTF-TCNQ.

A third basic problem is the possibility of usual pairing superconductivity and its relationship with the Peierls transition. This problem has been investigated extensively in the literature,[19,21-25] and we shall consider it within the discussion.

II. MODEL

In this section, we summarize the mean-field results for the one-dimensional case, and present our model for the interchain-coupling effect.

We start from the Fröhlich Hamiltonian

$$H = \sum_p \epsilon_p c_p^\dagger c_p + \sum_q \omega_q^0 a_q^\dagger a_q + \sum_{p,q} g_q (a_q + a_{-q}^\dagger) c_{p+q}^\dagger c_p \ , \tag{2.1}$$

where c_p, a_q are the electron and phonon destruction operators; ϵ_p, ω_q^0 are the electron and phonon unrenormalized energies; and g_q is the electron-phonon coupling constant.

We define a dimensionless coupling parameter s_q by

$$g_q^2 = s_q \omega_q^0 / 2N(0) \ , \tag{2.2}$$

$N(\epsilon)$ is the electron density of states for both spins, and $\epsilon = 0$ is the Fermi level. If v_F is the Fermi velocity, then $N(0) = 2/\pi a^2 v_F$, where a is the distance between chains, while c will denote the lattice constant along the chain.

The Hamiltonian (2.1) neglects direct electron-electron Coulomb interaction. Within the random-phase approximation (RPA),[17,19] the Coulomb effect renormalizes the electron-phonon coupling constant and thus amounts to a redefinition of the parameter s_q.

The one-dimensional Hamiltonian (2.1) was studied by many authors[6-8,14-19] using RPA calculations. The phonon with $q_z = 2p_F$ softens, and its frequency reaches zero at a temperature T_P. Below T_P, a superlattice with wave vector $2p_F$ appears, which introduces a gap in the electronic spectrum at $p = p_F$.

The phonon self-energy, within RPA is

$$\Pi_0(q, \omega, T) = -2g_q^2 \int \frac{d^3p}{(2\pi)^3} \frac{n_{p+q} - n_p}{\omega - (\epsilon_{p+q} - \epsilon_p) + i\delta} \ , \quad \delta = +0 \ , \tag{2.3}$$

where n_p is the electron momentum distribution function. T_P is the temperature where the phonon Green's function $D(q, \omega)$ has a pole at $\omega = 0$:

$$(\omega_q^0)^2 + 2\omega_q^0 \Pi_0(q, 0, T_P) = 0 \ .$$

For $T \ll T_F$, the instability occurs at $q_z = 2p_F$, although for $T \lesssim T_F$ this may not be the case.[15,17]

In general one deals with $T \ll T_F$, and we assume this to be the case throughout this work.

Let us define

$$\Pi_0(q, 0, T) = -s_q \omega_q I(q, T) \ , \tag{2.4}$$

where

$$I(q, T) = \tfrac{1}{2} v_F \left(\frac{a}{2\pi}\right)^2 \int d^3p \frac{n_p}{\epsilon_{p+q} - \epsilon_p} \ . \tag{2.5}$$

Thus T_P is obtained by solving

$$1 = 2sI(q_z = 2p_F, T_P) \ , \tag{2.6}$$

where s and ω_0 are the values of s_q and ω_q^0 at $q_z = 2p_F$.

Using a tight-binding spectrum $\epsilon_p = -\epsilon_F \cos p_z c$ for a half-filled band gives[16] $T_P = 2.26 T_F e^{-2/s}$. For a free-electron spectrum $\epsilon_p = p^2/2m$, and any filling of the band, the result is[8] $T_P = 4.52 T_F e^{-2/s}$. Later we shall use a free-electron spectrum, and for simplicity, an inclined step function for n_p. This gives a slight deviation, with the result[15]

$T_P = 2T_F e^{1-2/s}$.

In order to see the reason for the different coefficients, let us pass to integration on the energy variable. The use of electron-hole symmetry $\epsilon_{p+2p_F} = -\epsilon_p$ is valid for $p \simeq -p_F$, which is the important region of integration in (2.5). However, the energy integration implicitly includes both regions $p \simeq \pm p_F$, so that an extra factor of $\frac{1}{2}$ is needed to obtain from (2.3),

$$I(2p_F, T) = \frac{1}{8} \int \frac{N(\epsilon)}{N(0)} \tanh\left(\frac{\epsilon}{2T}\right) \frac{d\epsilon}{\epsilon} \quad . \tag{2.7}$$

This integral converges slowly, so that it depends on the form of $N(\epsilon)$, or alternatively, if we take $N(\epsilon) = N(0)$, the result depends on the electronic cutoff energy. However, the difference of $I(2p_F, T)$ at two temperatures does not depend on the cutoff. Using Eq. (2.6) we obtain

$$1/2s - I(2p_F, T) = \tfrac{1}{4} \ln T/T_P \; . \tag{2.8}$$

Our model for the interchain coupling involves electron hopping between the chains described by the electronic dispersion:

$$\epsilon_p = \epsilon(p_z) - \eta\epsilon_0(\cos a p_x + \cos a p_y) \; . \tag{2.9}$$

We define p_F as $\epsilon(p_z = p_F) = 0$ (see Fig. 1) and $v_F = \partial\epsilon(p_z = p_F)/\partial p_z$, so that $N(0)$ and s in (2.2) are formally defined as in the one-dimensional case. We also define

$$\epsilon_0 = \tfrac{1}{2} v_F p_F \; , \tag{2.10}$$

This energy coincides with ϵ_F only for the free-electron model. The Fermi surface which corresponds to (2.9) is shown in Fig. 1.

As we saw, the Fermi energy ϵ_F does not determine uniquely the energy scale in the problem. Indeed, the distance of the bottom of the band from the Fermi level is not a relevant quantity when we consider only states near the Fermi level. Thus, our scale of energy is determined only by Fermi-surface parameters as in (2.10).

The dispersion (2.9) corresponds to nearest neighbor tight binding in the transverse x, y directions, and η is the measure of the interchain coupling. Note that (2.9) implies a tetragonal lattice, but the extension to a triclinic lattice will be shown to be trivial.

Apart from the electronic dispersion, other quantities may depend on interchain coupling, such as g_q or ω_q^0. Within RPA calculations, this implies a dependence of the coupling parameter s_q on the transverse momenta. The consequences of such a dependence are straightforward, and we treat them in Secs. III and V.

For a three-dimensional dispersion, the equation for the Peierls instability instead of (2.6), is now

$$1 = 2s_{\vec{q}_0} I(\vec{q}_0, T_P) \; . \tag{2.11}$$

In Sec. III, we look for the value of a three-dimensional vector $\vec{q}_0$ which leads to the highest temperature of a Peierls instability. This corresponds to mean-field calculation, while fluctuation effects will be considered in Sec. IV.

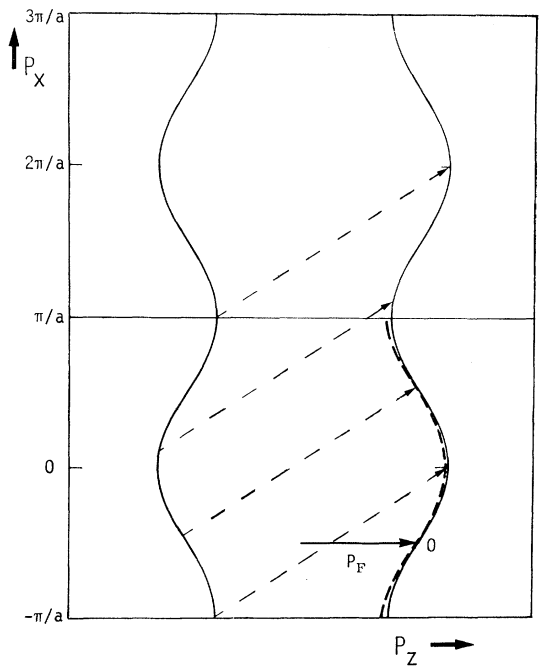

FIG. 1. Fermi surface following (2.9), (3.2) for $\eta = 0.5$ in the plane $p_y = \pi/2a$. Full line corresponds to $\alpha = 0$ and dashed line, to $\alpha = 1$. Note that for $\alpha \neq 0$, the symmetry across the point 0 is broken. For $\alpha = 0$, all the vectors $(\pi/a, \pi/a, 2p_F)$ connect opposite sides of the Fermi surface.

III. VALUE OF q_0

In this section we solve (2.11) for $\vec{q}_0$ and T, and show that if s_q is independent of $q_\perp$, the instability should occur at $q_0 \equiv (\pi/a, \pi/a, 2p_F)$ ($q_\perp$ stands for both q_x and q_y). We denote by s the value of s_q at $q = q_0$, and for comparison, by s_1 the value of s_q at $q_1 \equiv (0, 0, 2p_F)$. Even if s_q depends on $q_\perp$ and $s_1 > s$, we shall show it is possible that q_0 rather than q_1 describes the instability.

The basic difference between q_0 and q_1 can be noted by looking at Fig. 1. If $q_\perp = 0$, the vectors q_z which connect both sides of the Fermi surface are smeared around $q_z = 2p_F$ with a width of order $\eta \times 2p_F$. This peak around $2p_F$ is the cause of a giant Kohn anomaly, which for η smaller than some critical value η_c^1 (to be calculated here) will cause a Peierls instability. If $\eta > \eta_c^1$, the Kohn

anomaly is not strong enough and will not induce a Peierls instability with $q = q_1$. Let us now consider the case $q_\perp = \pi/a$, so that the instability is described by $q_0 = (\pi/a, \pi/a, 2p_F)$. Let us first assume electron-hole symmetry for $\epsilon(p_z)$. The Fermi surface is described by the full line in Fig. 1, and as shown, all the vectors q_0 connect opposite sides of the Fermi surface. In addition, all connected points on the Fermi surface have parallel tangents, which is the criterion for a Kohn anomaly.[26] Thus the Kohn effect is accumulated on the whole Fermi surface with the same wave vector q_0. The phonon with this wave vector sees an effectively one-dimensional system, although there is a finite (and possibly large) coupling between the chains. We may define such a Fermi surface as "effectively flat" with respect to the vector q_0. The degeneracy of all vectors q_0 connecting opposite sheets of the Fermi surface is due to inversion symmetry of the electron dispersion ϵ_p through the point $\vec{p} = \frac{1}{2}\vec{q}_0 = (p_F, \pi/2a, \pi/2a)$. To be more precise, we prove the following general assertion:

If there exists a point $\frac{1}{2}\vec{q}_0$ in the Brillouin zone such that

$$\epsilon(\tfrac{1}{2}\vec{q}_0 + \vec{p}) = -\epsilon(\tfrac{1}{2}\vec{q}_0 - \vec{p}) \tag{3.1}$$

and $\epsilon(\vec{p}) = \epsilon(-\vec{p})$, than there is a Peierls instability at a finite temperature associated with the wave vector $\vec{q}_0$. This result does not depend on the details of the electronic spectrum $\epsilon(\vec{p})$ (like the value of the interchain coupling), but only upon the validity of (3.1).

To prove our assertion, we note that the assumptions are equivalent to $\epsilon(\vec{p} + \vec{q}_0) = -\epsilon(\vec{p})$. Thus (2.5) reduces to (2.7) which has the one-dimensional singularity at $T = 0$.

The inversion symmetry (3.1) is essentially a particle-hole symmetry through the point $\frac{1}{2}\vec{q}_0$. For the dispersion (2.9), we obviously have $\frac{1}{2}\vec{q}_0 = (\pm\pi/2a, \pm\pi/2a, \pm p_F)$, and one such point is denoted by 0 in Fig. 1.

Let us now analyze when the relation (3.1) is expected to be valid. The first assumption is the use of nearest-neighbor tight binding, as in (2.9), for the dependence on the transverse components p_x, p_y. This is a reasonable assumption due to the relatively small interchain interaction. The second assumption is the use of electron-hole symmetry for $\epsilon(p_z)$, namely, $\epsilon(p_F + p_z) = -\epsilon(p_F - p_z)$. This is exact for the half-filled nearest-neighbor tight-binding dispersion, or more generally, if the expansion of $\epsilon(p_F + \delta p_z)$ contains only odd powers of δp_z. For $T \ll T_F$, we expect the linear term to be dominant, so that the second assumption is reasonable too. However, for large enough η, we expect some symmetry breaking effect due to the second-order term. Thus for actual calculations we use the following dispersion:

$$\epsilon(p_z) = \begin{cases} \epsilon_0[2\delta p_z/p_F + \alpha(\delta p_z/p_F)^2], & p_z > 0, \\ \epsilon_0[-2\delta p_z/p_F + \alpha(\delta p_z/p_F)^2], & p_z < 0, \end{cases} \tag{3.2}$$

$$\delta p_z = p_z - p_F, \qquad p_z > 0,$$

$$\delta p_z = p_z + p_F, \qquad p_z < 0.$$

We chose the coefficients so that $\epsilon_0 = \frac{1}{2} v_F p_F$ in accordance with (2.10), and $\alpha = 1$ corresponds to the free electron dispersion. Expanding the nearest-neighbor tight-binding dispersion gives $0 \leq \alpha \leq 1$, if the band is between zero and half-filled. If the band is more than half-filled, $2p_F > \pi/c$, and the instability should be described by $(2\pi/c - 2p_F)$. Alternatively, we may consider the Fermi vector $p'_F = \pi/c - p_F$ and obtain $-1 \leq \alpha \leq 0$. Although, in principle, it is possible to have $|\alpha| > 1$, the values of $|\alpha| = 1$ and $\alpha = 0$ represent the two physically extreme cases of the free electron dispersion ($\alpha = 1$) and the half-filled nearest-neighbor tight-binding dispersion ($\alpha = 0$). For KCP, the band is $\frac{5}{6}$ filled, so that for the hole spectrum $p_F = \pi/6c$ and $\alpha \simeq 0.9$. Part of the Fermi surface for $\alpha = 1$ is shown in Fig. 1 by the dashed line. The symmetry through the point 0 is broken, and the wave vectors $(\pi/a, \pi/a, q_z)$ connecting the Fermi surface do not have the same q_z. Therefore, the Kohn anomaly is smeared and we again expect a critical value η_c, such that for $\eta > \eta_c$, the Peierls transition is suppressed. Due to the preferred direction of q_0 we expect $\eta_c \gg \eta_c^1$.

Before presenting the detailed results, let us make two remarks. The choice of (2.9) with (3.2) is a reasonable simplification of an actual dispersion, but even for a more complicated dispersion, the symmetry $\epsilon(\vec{p}) = \epsilon(-\vec{p})$ alone ensures that the strength of the Kohn anomaly is largest for $q_\perp = (\pi/a, \pi/a)$. Obviously, the "effective flatness" of the Fermi surface is always highest for $q_\perp = (\pi/a, \pi/a)$. Thus if one has a possibility for a Peierls transition, it should *a priori* be associated with the wave vector q_0, as long as s_q does not decrease too much with $q_\perp$.

The second remark is the generalization of our treatment to a triclinic system. If $\vec{a}, \vec{b}, \vec{c}$ are the vectors of the unit cell, the equivalent of (2.9) is

$$\epsilon_{\vec{p}} = \epsilon(p_z) - \epsilon_0(\eta_1 \cos\vec{a}\cdot\vec{p} + \eta_2 \cos\vec{b}\cdot\vec{p}).$$

It can be easily checked that again, the transverse components of q_0 are at the corner of the Brillouin zone. If we choose the axes along the vectors of the reciprocal unit cell, then for $\epsilon(p_z)$

which has electron-hole symmetry, $q_0 = (\pi/a, \pi/b, 2p_F)$, which satisfies (3.1). However, as the system deviates more from the orthorombic structure, the second-neighbor effect becomes stronger. Since the transfer integrals in the z direction are the most important, the relation (3.1) is a good approximation only if we are rather close to a monoclinic structure.

Even then, second neighbors in the $(\vec{a}, \vec{b})$ plane may become important, until eventually, for the hexagonal lattice, there are three pairs of nearest neighbors in the transverse plane. In this case, ϵ_p has three equally important terms which depend on p_x, p_y, whence Eq. (3.1) implies three equations for q_{0x} and q_{0y}, so that there is no solution for q_0. In such a case, the dependence of s_q on $q_\perp$ will determine the wave vector of the instability.

A. $q_0 = (\pi/a, \pi/a, 2p_F)$

We evaluate $I(q, T)$ for $q = (\pi/a, \pi/a, 2p_F + q_z)$ with the dispersion (2.9) and (3.2) to lowest order in η. For $q_z \ll 2p_F$, we have

$$\epsilon_{p+q} - \epsilon_p = 2v_F[p_z + p_F + \tfrac{1}{2}\eta p_F(\cos ap_x + \cos ap_y) + \tfrac{1}{2}q_z] .$$

The limits of the Fermi surface $p_z = p_1(p_x, p_y)$ are given by

$$p_1 = p_F[1 + \tfrac{1}{2}\eta(\cos ap_x + \cos ap_y) - \tfrac{1}{8}\alpha\eta^2(\cos ap_x + \cos ap_y)^2 + O(\eta^3)] .$$

We change variables to $p_z' = p_z + p_1 - p_F$. The linear term in η cancels and from (2.5) we obtain

$$I(q, T) = \frac{1}{4}\left(\frac{a}{2\pi}\right)^2 \int_{-\pi/a}^{\pi/a} dp_x dp_y \int dp_z' \frac{n(\epsilon_{p'})}{p_z' + p_F + \frac{1}{2}p_F\alpha\eta^2(\cos ap_x + \cos ap_y)^2 + \frac{1}{2}q_z} . \tag{3.3}$$

The change of variables ensures that the drop of $n(\epsilon_{p'})$ from 1 to 0 is around $p_z' = -p_F$ for all p_x, p_y. (The behavior at $p_z' = +p_F$ is not important.)

For $T = 0$, (3.3) can be evaluated, with the result

$$I(0, 0) = -\tfrac{1}{2}\ln|\tfrac{1}{8}\eta(|\alpha|)^{1/2}| .$$

Thus from (2.11) we obtain

$$\eta_c = 8/(|\alpha|)^{1/2}e^{-1/s} \simeq 3.5(\tau_P^0/|\alpha|)^{1/2} , \tag{3.4}$$

where $\tau_P^0 = T_P(\eta = 0)/\epsilon_0$ and the coefficient 3.5 depends somewhat on the choice of the electronic cutoff as discussed for Eq. (2.6). The Peierls instability exists only for $\eta < \eta_c$, and as expected, there is no such limitation when $\alpha \to 0$.

For $T \neq 0$, we evaluate (3.3) in the appendix using an inclined step function for n_p. We plot $I(x, \tau)$ in the upper row of Fig. 2, where $x = q_z/2p_F$ and $\tau = T/\epsilon_0$. For a given η, the peak becomes higher and sharper as τ decreases, until for $\tau \lesssim \frac{1}{2}\alpha\eta^2$, the asymmetry term $\alpha\eta^2$ dominates, and further decrease of τ has a small effect on $I(x, \tau)$. Since $1/s = 2I(q, T_P)$, these curves can be viewed as a set of critical curves $s_c(\eta, q_z, T)$. For a given η, T, an instability will occur at the point where $s(q_z) \geq s_c(\eta, q_z, T)$. For $\tau \ll 1$, the sharpness of the peak indicates that the instability should occur at $(q_0 + q)_z = 2p_F$, but for $\tau \gtrsim 0.1$ the peak is broad, and some dependence $s(q_z)$ may cause an instability at a different q_z.

The asymmetry for $\alpha \neq 0$ causes a small shift from $x = 0$ to $x_m \simeq -\frac{1}{8}\alpha\eta^2$ (if $\tau \gtrsim |x_m|$) in the peak of $I(x, \tau)$. We solve the instability equation $1 = 2sI(x, \tau_P)$ with x at the peak and plot τ_P in Fig. 3. We conclude that $\tau_P(\eta)$ is almost constant until very close to the critical η_c, where it drops down to zero. [Due to approximations in the appendix, the values of η_c in Figs. 3 and 4 is somewhat less than the result (3.4)].

Higher-order terms in the η expansion and in the tight-binding scheme limit the validity of our results to small η. Since we use η to second order, we estimate the region of validity as $\eta^2 \lesssim 0.1$.

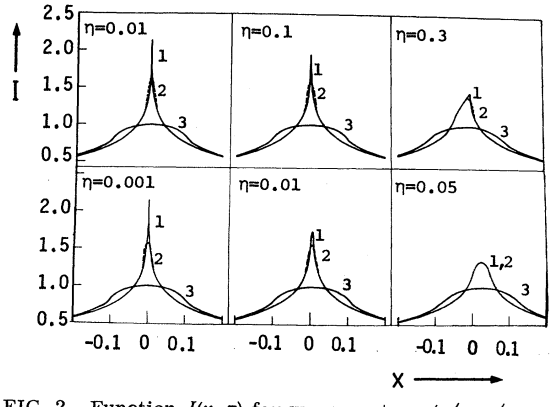

FIG. 2. Function $I(x, \tau)$ for wave vectors $(\pi/a, \pi/a, 2P_F + q_z)$ in the upper row, and for $(0, 0, 2p_F + q_z)$ in the lower row, using $\alpha = 1$; $x = q_z/2p_F$ and $\tau = T/\epsilon_0 \simeq T/T_F$. In each section, we plot three curves for $\tau = 0.001$ (1), 0.01 (2), and 0.1 (3).

B. $q_1=(0,0,2p_F)$

For comparison, we repeat the calculations of Sec. III A for the wave vectors $q=(0, 0, 2p_F+q_z)$. In this case: $\epsilon_{p+q}-\epsilon_p=2v_F(p_z+p_F+\frac{1}{2}q_z)$, and the change of variables to $p_z'=p_z+p_1-p_F$ gives a term linear in η:

$$I(q, T)=\frac{1}{4}\left(\frac{a}{2\pi}\right)^2\int\int dp_x dp_y \int dp_z' \frac{n(\epsilon_{p'})}{p_z'+p_F-\frac{1}{2}\eta p_F(\cos ap_x+\cos ap_y)+\frac{1}{2}q_z} \quad . \tag{3.5}$$

$T=0$ calculation gives $I(0, 0)=-\frac{1}{4}\ln|\frac{1}{8}\eta|$, whence

$$\eta_c^1=8e^{-2/s_1}\simeq 1.5\tau_P^0 \, . \tag{3.6}$$

This result is independent of α as expected, since the interchain coupling itself is responsible for the suppression of the Peierls instability at q_1. Also for $\tau_P^0\ll 1$, we have from (3.4) $\eta_c^1\ll\eta_c$, if $s=s_1$ as expected.

For $T\neq 0$, we evaluate (3.5) in the appendix, the way we did with (3.3). The result for $I(x, \tau)$ is shown in the lower row of Fig. 2. Evidently, the effect of η is much more drastic than in the case of q_0. Roughly, the results for a given η in the q_0 case correspond to the results with $\eta'=\frac{1}{2}\alpha\eta^2\ll\eta$ in the q_1 case. The solution for τ_P is shown by the dashed line in Fig. 3. We observe again a sharp depression of τ_P near $\eta=\eta_c^1$. Evidently, for $\eta_c^1\lesssim\eta\lesssim\eta_c$ only, the transition with q_0 exists.

Finally, let us discuss the effect of the $q_\perp$ dependence of s_q. If s_q does not depend on $q_\perp$, then the instability is always at $q_\perp=\pi/a$. For $\eta\lesssim\eta_c^1$, a small maximum of s_q at any value of $q_\perp$ will force the instability to have that value of $q_\perp$ [see Eq. (5.10)]. However, for $\eta\gtrsim\eta_c^1$, the transition with $q_\perp=0$ is suppressed, and we should check transitions with other values of $q_\perp$. For any $q_\perp$ in the range $0\leq q_\perp<\pi/a$, there is no "effective flatness," and there is some finite η_c, even if $\alpha=0$, like in (3.6). Thus for $\eta>\max\eta_c(q_\perp)$, all transitions are suppressed except for $q_\perp=\pi/a$, if α is small enough. Comparison of (3.6) and (3.4) shows that the transition with $q_\perp=0$ will dominate that for $q_\perp=\pi/a$ for all η only if s_1 is large enough compared with s:

$$s_1\gtrsim 2s/(1+\tfrac{1}{2}s\ln|\alpha|) \tag{3.7}$$

and for $\alpha=1$, this implies $s_1\gtrsim 2s$. Thus we conclude that for $\eta\gtrsim\eta_c^1\sim\tau_P^0$, the instability with $q_\perp=\pi/a$ is strongly favored. As we shall see in Sec. IV, roughly the same region ensures small fluctuation effects, so that the mean-field calculation that we use for q_0 is valid in that region.

IV. FLUCTUATIONS

In this section we investigate the effect of fluctuations on the temperature of the Peierls transition. We denote by T_P^0 the results of mean-field theory as obtained in Sec. III A for $\vec{q}_0=(\pi/a, \pi/a, 2p_F)$, and look for the real transition temperature T_P.

We are interested in the region with $T_P^0\neq 0$, and

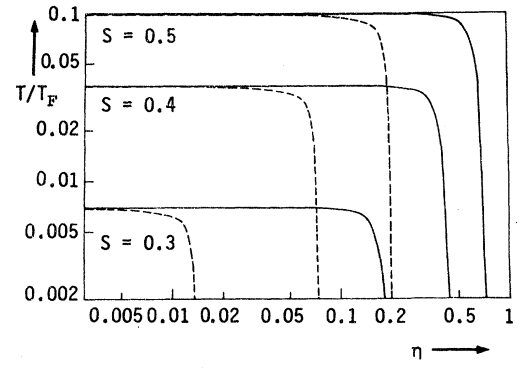

FIG. 3. Mean-field Peierls transition temperatures for the dispersion (2.9), (3.2) with $\alpha=1$. Full line is the transition temperature for the $q_0=(\pi/a, \pi/a, 2p_F)$ instability, and dashed line for the $q_1=(0, 0, 2p_F)$ instability. The electron-phonon coupling constant is given by s.

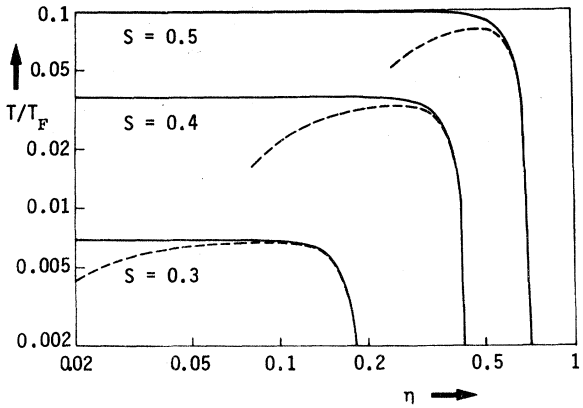

FIG. 4. Peierls transition temperature including fluctuations (dashed line) for the instability at q_0. Full line is the mean-field transition temperature. The electron-phonon coupling constant is given by s, and $\alpha=1$ in the dispersion (3.2).

as we saw in Fig. 3, until very close to the critical η_c, $T_P^0(\eta)$ is almost flat. Roughly for $\eta \lesssim 3(\tau_P^0/|\alpha|)^{1/2}$, the asymmetric effect due to $\alpha \neq 0$ in (3.2) is negligible, and $T_P^0 \simeq T_P^0(\eta=0)$.

In order to calculate fluctuation effects, we need the expansion of $I(q, T)$ for $\vec{q}_0+\vec{q} = (\pi/a+q_x, \pi/a+q_y, 2p_F+q_z)$. From (2.9) and (3.2), we obtain the result (3.3), except for the replacement $q_z \to Q(\vec{q}, p_x, p_y)$, where

$$\begin{aligned} Q(\vec{q}, p_x, p_y) &= q_z - \tfrac{1}{2}\eta p_F[\cos ap_x(1-\cos aq_x) \\ &\quad + \sin ap_x \sin aq_x + \cos ap_y(1-\cos aq_y) \\ &\quad + \sin ap_y \sin aq_y] \ . \end{aligned} \tag{4.1}$$

We may use the one-dimensional expansion[14] for the dp_z' integration in (3.3),

$$I(q_z, T) = I(0, T) - \tfrac{7}{16}\zeta(3)(v_F q_z/2\pi T)^2 + O(q_z^4) \ . \tag{4.2}$$

This expansion is valid for $q_z \lesssim 2\pi T/v_F$. The term with α in (3.3) does not depend on $\vec{q}$ and causes just a small shift in the q_z peak position as discussed in III A. This is not important here, so that in (4.2) we just perform the replacement (4.1) and the necessary averaging $(a/2\pi)^2 \times \int\int Q^2(\vec{q}, p_x, p_y)dp_x dp_y$.

For brevity we use $7\zeta(3)=8$ and obtain

$$I(q, T) = I(0, T) - \tfrac{1}{2}(v_F/2\pi T)^2 \times [q_z^2 + \tfrac{1}{2}\eta^2 p_F^2(\sin^2\tfrac{1}{2}aq_x + \sin^2\tfrac{1}{2}aq_y)] . \tag{4.3}$$

Expanding to second order in q_x, q_y we find that this result is valid for

$$q_z^2 + \tfrac{1}{8}\eta^2 p_F^2 a^2 q_\perp^2 \lesssim (2\pi T/v_F)^2 \ , \tag{4.4}$$

where $q_\perp^2 = q_x^2 + q_y^2$.

The fluctuations in the ions position $\langle u^2\rangle$ can be evaluated using the fluctuation-dissipation theorem. (For a detailed derivation, see Sec. VII of Ref. 15). For the gap Δ, we have $\Delta^2 = u^2 sMN\omega_0^2/N(0)$, where M, N are the mass and density of the ions, whence the fluctuation of the gap is

$$\langle\Delta^2\rangle = \frac{T}{16\pi^3 N(0)} \int \frac{d^3q}{1/2s - I(q, T)} \ . \tag{4.5}$$

Using (2.8), we obtain

$$\langle\Delta^2\rangle = \frac{T}{4\pi^3 N(0)} \times \int \frac{d^3q}{\ln(T/T_P^0) + 2(v_F/2\pi T)^2(q_z^2 + \frac{1}{8}\eta^2 p_F^2 a^2 q_\perp^2)} \tag{4.6}$$

The region of integration is limited by the Brillouin zone and by (4.4). The limit imposed by (4.4) means that the contributions to (4.6) outside this limit are negligible. Physically, this implies that the thermal energy restricts the important fluctuations to be in the region (4.4), and as the temperature is lowered, this region becomes smaller. We may define two cutoff lengths so that $\pi/\xi_{\parallel,\perp}^0$ is the limit (4.4) on q_z or $q_\perp$ separately:

$$\xi_\parallel^0 = v_F/2T \ ; \ \xi_\perp^0 = a\eta/8^{1/2}\tau \ , \tag{4.7}$$

where $\tau = T/\epsilon_0 = T/\frac{1}{2}v_F p_F$ as before. Generally, $\xi_\parallel^0 \gg a$, but not so for $\xi_\perp^0$. If $\xi_\perp^0 < a$, the transverse fluctuations are restricted only by the Brillouin-zone limit. However, if $\xi_\perp^0 > a$, the limit (4.4) is inside the Brillouin zone, and fluctuation effects are reduced in an essential way. We expect that a phase transition can happen only in such a case, namely,

$$T_P \lesssim T_2 = \tfrac{1}{4}\eta\epsilon_0 \ . \tag{4.8}$$

[The factor 4 replaces $8^{1/2}$ if, in the limit of $q_x = \pi/a$, we avoid the expansion of (4.4)].

The condition (4.8) determines the usefulness of the mean-field transition temperature. If $T_P^0 \lesssim T_2$, fluctuation effect on the transition temperature should be small, and we shall confirm this explicitly. This means that already at $T = T_P^0$, the interchain energy ($\sim\eta\epsilon_0$) is enough to suppress thermal fluctuations. On the other hand, if $T_P^0 \gg T_2$, (4.8) implies a strong reduction in the temperature before the interchain coupling is sufficient to induce a three-dimensional phase transition.[27] In this case, fluctuations should be treated to higher orders, which are not considered in the present work. Thus T_2 is a basic temperature of the system, and the possibility that the mean-field temperature is relevant is a mere chance, whether T_P^0 (which is determined by s) falls above or below T_2.

We proceed to evaluate $\langle\Delta^2\rangle$ for the two cases: η small ($\eta \lesssim 4\tau$) and η large ($\eta \gtrsim 4\tau$). For small η, the integration limit in (4.6) is an ellipsoid truncated by the Brillouin zone in the q_x, q_y directions. We approximate these limits by $|q_z| \lesssim 2\pi T/v_F$, $q_\perp^2 < 4\pi/a^2$ and obtain

$$\langle\Delta^2\rangle = \pi^3\sqrt{2}\,T^2\frac{\tau^2}{\eta^2}\left[\left(\ln\frac{T}{T_P^0} + \frac{\eta^2}{\pi\tau^2}\right)^{1/2} - \left(\ln\frac{T}{T_P^0}\right)^{1/2}\right] . \tag{4.9}$$

Let us define the temperature T_1 by the relation

$$\ln T_1/T_P^0 = \eta^2/\pi\tau_1^2 \ . \tag{4.10}$$

For $T \gg T_1$, expanding (4.9) we obtain

$$\langle\Delta^2\rangle = \pi^2 T^2/[2\ln(T/T_P^0)]^{1/2} \quad (T \gg T_1) \ . \tag{4.11}$$

This is the one-dimensional result which diverges at T_P^0. However as T approaches T_P^0, the interchain coupling dominates, and finally

$$\langle\Delta^2\rangle = \pi^2 T^2 (2\pi)^{1/2}\tau/\eta, \quad (T = T_P^0) . \tag{4.12}$$

Thus T_1 defines a temperature where the system passes from a one- to three-dimensional behavior.

We evaluate the actual transition temperature using the Orenstein-Zernike criterion,

$$\langle\Delta^2\rangle_{T=T_P^0} = \bar{\Delta}^2_{T=T_P}, \tag{4.13}$$

where $\bar{\Delta}$ is the actual gap in mean-field theory. (We shall later discuss the validity of this criterion.) Mean-field theory gives[14]

$$\bar{\Delta}^2 = -10T^2 \ln(T/T_P^0) . \tag{4.14}$$

Thus from (4.12) and (4.13) we obtain

$$\ln(T_P/T_P^0) = -2.5\tau_p^0/\eta . \tag{4.15}$$

Since we deal with $\eta \lesssim 4\tau$, (4.15) implies a large shift, and we do not expect mean-field theory or the result (4.15) to be valid. In this case, specific higher-order diagrams should be considered. For example, the RPA bubble diagram with dressed electron lines gives[28] $T_P \sim (c)^{1/2} T_P^0$ in the limit of small c, where c is the anisotropy in the phonon dispersion. The difficulty in such calculations is the fact that for small interchain coupling, the whole perturbation expansion diverges,[29] and one should be cautious in selecting the correct diagrams.

Consider now the case of large $\eta, \eta \gtrsim 4\tau$. The integration limits in (4.6) are determined by the ellipsoid (4.4). We can change to spherical coordinates and end up with

$$\langle\Delta^2\rangle = 4\pi^2 T^2 \frac{\tau^2}{\eta^2} \times\left[1 - \left(\tfrac{1}{2}\ln\frac{T}{T_P^0}\right)^{1/2} \tan^{-1}\left(\frac{2}{\ln T/T_P^0}\right)^{1/2}\right] . \tag{4.16}$$

Note that "large" or "small" η depends on temperature. If η is "large" near T_P^0 ($\eta \gtrsim 4\tau_P^0$), at higher temperatures ($T > T_2$) we pass to the region of "small" η, and finally above T_1, as defined in (4.9), we pass to the one-dimensional region. Usually one has, indeed, $T_1 > T_2$, since $T_1 < T_2$ implies by (4.8) and (4.10) that $\eta \gtrsim 4\times 10^3 \tau_P^0$, which is not reasonable for actual systems.

Use of the criterion (4.13) leads now to

$$\ln T_P/T_P^0 = -4(\tau_P^0/\eta)^2 . \tag{4.17}$$

Since $\eta \gtrsim 4\tau_P^0$, we obtain $0.8T_P^0 \lesssim T_P < T_P^0$, whence a maximal shift of 20% in the transition temperature. This is a small shift and confirms our expectation that for $\eta \gtrsim 4\tau_P^0$, mean-field theory is valid. T_P and T_P^0 are plotted in Fig. 4, and evidently for smaller τ, we obtain a larger range of η with a small shift. Using (3.4), we conclude that one dimensional mean-field theory is effectively valid in the region

$$4\tau_P^0 \lesssim \eta \lesssim 3(\tau_P^0/|\alpha|)^{1/2} . \tag{4.18}$$

This relation is the basic result of the present work. It gives the region of interchain coupling where one-dimensional theories based on mean-field approximation (and such are most of the available theories[6-8,14-19]) are applicable. The result (4.18) is due to a remarkable property of the RPA bubble diagram. This diagram feels only two bare electronic states at a time and so can be effectively one dimensional for a dispersion which satisfies (3.1). On the other hand, higher-order diagrams feel more electronic states at a time and cannot be effectively one dimensional. This is precisely the reason why we can have a mean-field theory which is effectively one dimensional, and still have small fluctuation effects.

V. APPLICATIONS

In this section we evaluate the neutron-scattering cross section and the specific heat and compare with experimental results. Neutron-scattering experiments give direct information on the phonon-spectral density distribution $B(q, \omega)$, and thus can sensitively detect the approach to a Peierls instability.

Neutron-scattering experiments on KCP[13] have shown softening of the acoustic phonon with wave vector $q_0 = (\pi/a, \pi/a, 2p_F)$, although actual phase transition was not established. It is possible that disorder of the Br ions or the K atoms inhibits the occurrence of a phase transition.

An alternative explanation[17] for the instability at q_0 for KCP, suggests that Coulomb screening leads to a maximal s_q at $q = q_0$. This effect may exist together with our model for the band structure, and thus favor more strongly the transition at q_0.

The neutron cross section in the Born approximation is given by[30]

$$S(q, \omega) \sim B(q, \omega)/(e^{\omega/T} - 1) . \tag{5.1}$$

In order to compare our results with experiment, we must note that the experimental energy resolution was larger than the width of the central peak.[13] Thus, we may use the sum rule

$$\int_0^\infty \frac{1}{\omega} B(q, \omega) = [\omega_0 + 2\Pi_0(q, 0, T)]^{-1} \tag{5.2}$$

to obtain from (5.1) the integrated cross section around the central peak

$$S(q)\sim T\{\ln(T/T_P^0)+7\xi(3)(v_F/4\pi T)^2 \times[q_z^2+\tfrac{1}{2}\eta^2 p_F^2(\sin^2\tfrac{1}{2}aq_x+\sin^2\tfrac{1}{2}aq_y)] +2/s_q-2/s_{q_0}\}^{-1}. \quad (5.3)$$

If the variation of s_q with q can be neglected, taking $7\xi(3)=8$, the correlation lengths are identified as

$$\xi_{\parallel}=v_F/\pi T[2\ln(T/T_P^0)]^{1/2}, \qquad \xi_{\perp}=\eta a/2\pi\tau[\ln(T/T_P^0)]^{1/2}. \quad (5.4)$$

In Fig. 5, we compare the critical scattering at q_0 – $S(0)$ and $\xi_{\perp}$ with the experimental values.[13] We obtain a fit with $T_P^0=107\,^{\circ}\mathrm{K}$ and interchain energy coupling of $\eta\epsilon_0=300\,^{\circ}\mathrm{K}$. A possible dependence of S_q on $q_{\perp}$ is actually absorbed in the fitted value of η. The fit is reasonable for $110\,^{\circ}\mathrm{K}\lesssim T$, while for lower temperatures, the phase transition is not completed as mentioned above. For $T\gtrsim 140\,^{\circ}\mathrm{K}$ $S(0)$ overestimates the experimental values, because then the central peak does not dominate the integral (5.2), and we overestimate it by taking the integration limit to infinity.

From the fit we obtain $\eta/\tau_P^0\simeq 3$, which is somewhat below the region (4.18) of small fluctuations. We conclude that fluctuation effects are important for KCP, although they do not have a drastic effect, as is evident from the comparison of mean-field theory with experiment in Fig. 5.

Let us now evaluate the fluctuation effect on the specific heat. The thermodynamic potential due to interactions is given within RPA by[30]

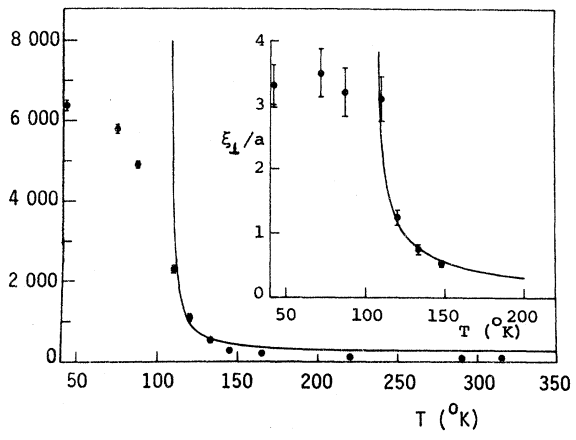

FIG. 5. Critical neutron-scattering cross section at $q_0=(\pi/a,\pi/a,2P_F)$, using $T_P^0=107\,^{\circ}\mathrm{K}$. The inset shows the transverse correlation length using $T_P^0=107\,^{\circ}\mathrm{K}$ and interchain coupling energy of $\eta\epsilon_0=300\,^{\circ}\mathrm{K}$. The experimental points are from Renker *et al.* (Ref. 13). For discussion, see Sec. V.

$$\Omega_1=-T\sum_n\int_0^1\frac{d\lambda}{\lambda}\int\frac{d^3q}{(2\pi)^3}\,\tfrac{1}{2}\lambda\Pi_0(q,\omega_n)D(q,\omega_n), \quad (5.5)$$

where $\omega_n=2\pi Tn$ and $D(q,\omega_n)=-2\omega_0/[\omega_n^2+\omega_0^2+2\omega_0\lambda\Pi_0(q,\omega_n)]$. Retaining only the most important term $n=0$, we obtain

$$\Omega_1=\frac{T}{2(2\pi)^3}\int\ln[1-2sI(q,T)]d^3q. \quad (5.6)$$

Using (4.3) and the integration limits (4.4), we obtain for the specific heat per electron

$$C_1=-T\frac{\partial^2}{\partial T^2}\Omega_1=\frac{\pi^2T^3}{8\eta^2}\frac{\tan^{-1}[2/\ln(T/T_P^0)]^{1/2}}{[\frac{1}{2}\ln(T/T_P^0)]^{1/2}}. \quad (5.7)$$

There are other terms in the result for C_1 which are smooth functions of temperature. Usually smooth backgrounds are subtracted from the experimental results so that (5.7) should apply.

The result (5.7) diverges at T_P^0, however, very near T_P^0, renormalization effects are important and (5.7) is not valid.

Specific-heat measurements have been carried out on TTF-TCNQ[31] showing a rise from $T\simeq 60\,^{\circ}\mathrm{K}$ up to a peak at $53\,^{\circ}\mathrm{K}$. Entropy conservation gives[31] $T_P\simeq 55\,^{\circ}\mathrm{K}$. Equation (5.7) gives a reasonable fit somewhat above $55\,^{\circ}\mathrm{K}$ with $\eta\simeq 0.1$ and $\tau=0.025$ ($T_F\simeq 0.2$ eV). However, the experimental results for C_1 are not exact due to the uncertainty in the background subtraction.

Some more insight into our case can be made by the free-energy expansion

$$F(\Delta,T)=-T\sum_p\ln(1+e^{-E_p/T})+\frac{N(0)}{S}\Delta^2. \quad (5.8)$$

The first term is the electronic free energy, and the second is the elastic energy of the distorted lattice. Using the dependence of E_p on Δ_q[15] we obtain

$$F(\Delta,T,q)=N(0)\{[1/s-2I(q,T)]\Delta_q^2+0.026\Delta^4/T^2\}. \quad (5.9)$$

Finally, using (4.3) and (2.8) we have

$$F(\Delta,T,q)=\tfrac{1}{2}N(0)\left[\ln\left(\frac{T}{T_P^0}\right)+\frac{2}{s_q}-\frac{2}{s}+2\left(\frac{v_F}{2\pi T}\right)^2 \times[q_z^2+\tfrac{1}{2}\eta^2p_F^2(\sin^2\tfrac{1}{2}aq_x+\sin^2\tfrac{1}{2}aq_y)]\right]\Delta_q^2+0.026N(0)\frac{\Delta^4}{T^2}. \quad (5.10)$$

We note that $\vec{q}$ is measured from the instability wave vector $\vec{q}_0=(\pi/a,\pi/a,2p_F)$ and $s=s_{q_0}$. The terms involving $\vec{q}$ represent the excess energy required to create a gap with a wave vector different than q_0. We observe that if s is independent

of $q_\perp$, then the free energy has a minimum at $q_\perp = 0$ and a maximum at $q_\perp = \pi/a$. In order to produce a gap at $q_\perp \neq 0$, the coupling s_q should behave in an opposite way and compensate for the excess energy.

The expansion (5.10) is suitable for use of the renormalization group techniques. Thus the first order shift in the transition temperature can be evaluated,[32] and it turns out that the criterion (4.13) is equivalent to this first-order term up to a factor of $\frac{2}{3}$, which has a small effect on our results.

An interesting feature in (5.10) is that the transverse coupling is quadratic in η, which leads to much stronger fluctuation effect than a linear dependence. Alexander and Amit[33] have estimated fluctuation effects based on a free-energy expansion similar to (5.10). They obtain an analogous result to (4.17), but assume that the coefficient of $q_\perp^2$ is measured by the interchain coupling η. If this could be the case, the temperature shift would be small in the region $\tau^2 \lesssim \eta$ which is much larger than the region in (4.18).

VI. DISCUSSION

Up to date the only experimentally established Peierls transition is found in KCP. X rays[12] and neutron scattering[13] experiments have shown that the instability is associated with the wave vector $q_0 = (\pi/a, \pi/a, 2p_F)$. We discussed this instability in Sec. V; however, additional effects due to diffusion processes and lattice defects[34] should be considered.

Another quasi-one-dimensional system is TTF-TCNQ. There, pressure dependence[35,36] of the conductivity is much weaker than in KCP,[37] especially near the transition. Thus it is possible that in this case we are in the region (4.18) of small fluctuations. We obtained from the specific-heat data in Sec. V the estimate $\eta \simeq 0.1$ for $\tau_P^0 = 0.025$, which is indeed within the region (4.18). Low-temperature properties[38] show a direct gap of $\Delta \simeq 90\,^\circ$K which is consistent with the mean-field result. Also, microwave measurements above the transition give $\eta \simeq 0.07$ [see Fig. 15, and Eq. (21) of Ref. 38]. TTF-TCNQ has a sharp metal to insulator transition near 58 °K, and together with the specific-heat data, a second-order phase transition is well established. Thus it is possible that we have here a Peierls transition, but it is not certain. X-ray measurements[39] could not show a static distortion in the lattice. Since the distortion amplitude is proportional to $1/\omega_0$, it is possible that a high-frequency phonon is responsible for the instability, and the distortion is too small to be observed. (For the $C \equiv N$ bond vibration the distortion is ~0.001 Å compared to ~0.01 Å for the acoustic phonon.) Reflectivity measurements[40] showed a broad minimum around 1500 cm^{-1} which was related to the optical phonon of the $C \equiv N$ band at 2100 cm^{-1}.[41] Such a high-frequency phonon, when leading to a Peierls instability, has in addition to the soft mode, a high-frequency branch somewhat below ω_0.[15] Thus if the $C \equiv N$ vibration is responsible for the Peierls transition in TTF-TCNQ, its high-frequency branch is shown to cause exactly the observed dip in the reflectivity.[41] Actually in the x-ray study[39] at 100 °K, only the $C \equiv N$ bond was observed to change compared to the room-temperature data.

Conductivity measurements show a peak just above the metal to insulator transition, which has typically[11,42] the value $\sigma/\sigma_{RT} = 20$–50. This peak was attributed to BCS-type fluctuations,[11] to Fröhlich-type fluctuations,[14] or even not connected at all with the transition near 58 K.[42] In a separate work,[43] we investigate the interchain coupling effect on the Fröhlich-type superconductivity fluctuations. We show that the high-frequency phonon model with $\eta \simeq 0.1$ gives a better agreement with experiment.

In conclusion, a Peierls instability due to the $C \equiv N$ bond vibration is consistent with experiments on TTF-TCNQ, but further experiments are needed to establish this and the meaning of the conductivity peak.

Still another quasi-one-dimensional system is the $A15$ intermetallic compounds.[3] The theory of Gor'kov[44] describes the possible martenisitic transformation in the $A15$ as a Peierls transition. In this case η may be large and even comparable with the critical η_c for the σ band.[3]

We proceed with a comment on the possibility of BCS-type superconductivity, and its relationship with the Peierls instability. The one-dimensional problem has been considered recently,[19,21-24] however the superconducting transition is not restricted to one-dimensional systems,[45] as is the Peierls transition. Thus, at least for $\eta > \eta_c$ [Eq. (3.4)], only the BCS transition occurs. In fact, if we are close enough to η_c from above, there is no Peierls instability, but a significant Kohn anomaly is still present. The Kohn anomaly leads to softer phonons, and for $\omega_0 \gg T_c$, this will lead to higher transition temperatures T_c.[25] For the $A15$, we may have $\eta \sim \eta_c$, and so it is possible that the high T_c of the $A15$ compounds is due in part to such a mechanism.

To summarize, our model for the band structure classifies the systems capable of undergoing a Peierls transition to three qualitatively different regimes:

(i) $\eta \lesssim 4\tau_P^0$: Mean-field theory is not valid,

strong fluctuation effects. [Unless other types of interchain couplings are important, e.g., Coulomb effects, and s_q of Eq. (2.2) has a strong dependence on $q_\perp$.]

(ii) $4\tau_P^0 \lesssim \eta \ll 1$ [or Eq. (4.18)]: one-dimensional mean-field theory is effectively valid, $T_P(\eta)$ can be approximated by $T_P^0(0)$ (i.e., calculated by assuming the system to be one dimensional, but neglecting fluctuations).

(iii) $\eta \simeq 1$: Peierls transition is suppressed.

TTF-TCNQ seems to belong to region ii, and KCP may be a borderline case between regions i and ii. The $A15$'s seem to be a borderline case between regions ii and iii, at least for the σ-band.

If a high T_c is associated with the one-dimensional electron-phonon interaction, and since fluctuations reduce transition temperatures (which is undersirable), it seems that the search for the possibility of high T_c, both theoretically and experimentally, should be concentrated in the region ii.

ACKNOWLEDGMENTS

We acknowledge stimulating and helpful discussions with S. Alexander, D. J. Amit, T. Maniv, D. J. Scalapino, and B. Halperin.

APPENDIX

We evaluate (3.3) using an inclined step function for n_p. The dp_z' integration is the same as in the one-dimensional case [Eq. (6.3) of Ref. 15]; thus

$$I(x,\tau) = (-1/8\tau)(a/2\pi)^2[|J(x+\tau) - J(x-\tau)] + \tfrac{1}{4}(1+\ln 2)\,, \tag{A1}$$

where $\tau = T/\epsilon_0$, $x = q_z/2p_F$, and

$$J(a) = \iint_{-\pi/a}^{\pi/a} dp_x dp_y [a + \tfrac{1}{8}\alpha\eta^2(\cos ap_x + \cos ap_y)^2] \times \ln|a + \tfrac{1}{8}\alpha\eta^2(\cos ap_x + \cos ap_y)^2|\,. \tag{A2}$$

Transforming to $u = \cos ap_x + \cos ap_y$, and $v = \sin ap_x + \sin ap_y$, we obtain

$$J(a) = 16\int_0^1 du\, K'(u)(a + \tfrac{1}{2}\alpha\eta^2 u^2)\ln|a + \tfrac{1}{2}\alpha\eta^2 u^2|\,. \tag{A3}$$

$K'(u)$ is a complete elliptic function of the first kind, and we use the expansion

$$K'(u) = \ln 4 - \ln u + O(u^2 \ln u)\,.$$

The integral with the $\ln u$ term is approximately proportional to the integral multiplying the $\ln 4$ term. The approximation is good for small η, and thus is consistent with our evaluation which is to lowest order in η.

If the proportionality constant is C, the result contains a factor $(\ln 4 + C)$. We fix C so that for $\eta \to 0$, we have the one-dimensional result; thus $C = \frac{1}{4}\pi^2 - \ln 4 \simeq 1.08$. In the other limit, $a \to 0$, evaluation of $J'(0)$ shows that C is indeed close to 1 for small η. For $\alpha = 1$, we obtain $C(\eta = 0.1) = 1.3$ and $C(\eta = 0.01) = 1.2$. Thus the final result is (apart from an additive constant which does not depend on a)

$$J(a) = 4\pi^2\left[(a + \tfrac{1}{6}\alpha\eta^2)\ln|a + \tfrac{1}{2}\alpha\eta^2| - \tfrac{4}{3}a + \tfrac{2}{3}a\left(\left|\frac{2a}{\alpha\eta^2}\right|\right)^{1/2}\ln\left|\frac{1 + (-2a/\alpha\eta^2)^{1/2}}{1 - (-2a/\alpha\eta^2)^{1/2}}\right|\right]. \tag{A4}$$

For $a/\alpha > 0$, the second "ln" should be replaced by $2\tan^{-1}(\alpha\eta^2/2a)^{1/2}$.

Evaluation of (3.5) proceeds on the same lines: (A1) is valid with the definition

$$J(a) = \iint_{-\pi/a}^{\pi/a} dp_x dp_y [a - \tfrac{1}{2}\eta(\cos ap_x + \cos ap_y)] \times \ln|a - \tfrac{1}{2}\eta(\cos ap_x + \cos ap_y)|\,. \tag{A5}$$

Using the same constant C, we obtain

$$J(a) = -(2\pi^2/\eta)[(a-\eta)^2 \ln|a-\eta| - 2a^2\ln|a| + 2a\eta]\,. \tag{A6}$$

---

*Supported by the U. S. Israel Binational Science Fund.

[1]For a review, see I. F. Shchegolev, Phys. Status Solidi A 12, 9 (1972).

[2]For a review, see H. R. Zeller, in *Advances in Solid State Physics* (Pergamon, New York, 1973), Vol. 13, p. 31.

[3]For a review, see M. Weger and I. Goldberg, in *Solid State Physics* (Academic, New York, 1973), Vol. 28, p. 1.

[4]B. G. Silbernagel, M. Weger, and E. S. Greiner, Phys. Rev. Lett. 13, 521 (1964); J. F. McEnvoy, Physica (Utr.) 55, 540 (1971).

[5]V. Hoffstein and R. W. Cohen, Phys. Lett. A 29, 603 (1969); M. Weger, Solid State Commun. 9, 107 (1971).

[6]R. E. Peierls, *Quantum Theory of Solids* (Oxford U. P., London, 1953), p. 108.

[7]H. Fröhlich, Proc. R. Soc. A 223, 296 (1954).

[8]C. G. Kuper, Proc. R. Soc. A 227, 214 (1955).

[9]P. A. Lee, T. M. Rice, and P. W. Anderson, Solid State Commun. 14, 703 (1974).

[10]A. N. Bloch, R. B. Weisman, and C. M. Varma, Phys. Rev. Lett. 28, 753 (1972).
[11]M. J. Cohen, L. B. Coleman, A. F. Garito, and A. J. Heeger, Phys. Rev. B 10, 1298 (1974); L. B. Coleman, M. J. Cohen, D. J. Sandman, F. G. Yamagishi, A. F. Garito, and A. J. Heeger, Solid State Commun. 12, 1125 (1973).
[12]R. Comes, M. Lambert, H. Launois, and H. R. Zeller, Phys. Rev. B 8, 571 (1973).
[13]B. Renker, L. Pintschovious, W. Glaser, H. Rietschel, R. Comes, L. Liebert, and W. Drexel, Phys. Rev. Lett. 32, 836 (1974).
[14]D. Allender, J. W. Bray, and J. Bardeen, Phys. Rev. B 9, 119 (1974).
[15]B. Horovitz, M. Weger, and H. Gutfreund, Phys. Rev. B 9, 1246 (1974).
[16]M. J. Rice and S. Strässler, Solid State Commun. 13, 125 (1973).
[17]A. Bjelis, K. Saub, and S. Barisic, Nuovo Cimento B 23, 102 (1974); see also, A. Madhukar, Solid State Commun. 15, 921 (1974).
[18]G. Beni, Solid State Commun. 15, 269 (1974); see also, W. Dieterich, A. Phys. 270, 234 (1974).
[19]K. Levin, D. L. Mills, and S. L. Cunningham, Solid State Commun. 15, 705 (1974).
[20]P. A. Lee, T. M. Rice, and P. W. Anderson, Phys. Rev. Lett. 31, 462 (1973).
[21]A. Bychkov, L. P. Gor'kov, and I. E. Dzyaloshinskii, Zh. Eksp. Teor. Fiz. 50, 738 (1966) [Sov. Phys.-JETP 23, 489 (1966)].
[22]H. Gutfreund, B. Horovitz, and M. Weger, J. Phys. C 7, 383 (1974).
[23]A. Birenboim and H. Gutfreund. J. Phys. Lett. 35, L147 (1974).
[24]M. J. Rice and S. Strässler, Solid State Commun. 13, 697 (1973).
[25]G. Bergmann and D. Rainer, Z. Phys. 263, 59 (1973).
[26]W. Kohn, Phys. Rev. Lett. 2, 393 (1959).
[27]G. Toulouse, Nuovo Cimento B 23, 234 (1974); S. Barisic and K. Uzelac (unpublished).
[28]M. J. Rice and S. Strässler, Solid State Commun. 13, 1389 (1974).
[29]A. M. Alfanas'ev and Yu Kagan, Zh. Eksp. Teor. Fiz. 43, 1456 (1962) [Sov. Phys.-JETP 16, 1030 (1963)].
[30]A. A. Abrikosov, L. P. Gorkov, and I. E. Dzyaloshinski, *Methods of Quantum Field Theory in Statistical Physics* (Prentice-Hall, Englewood Cliffs, N. J., 1963).
[31]R. A. Craven, M. B. Salamon, G. DePasqualli, R. M. Herman, G. Stucky, and A. Schultz, Phys. Rev. Lett. 14, 769 (1974).
[32]D. J. Amit, J. Phys. C 7, 3369 (1974).
[33]S. Alexander and D. J. Amit (unpublished).
[34]J. Bernasconi, D. Kuse, M. J. Rice, and H. R. Zeller, J. Phys. C 5, L-127 (1972).
[35]C. W. Chu, S. M. E. Harper, T. H. Geballe, and R. L. Greene, Phys. Rev. Lett. 31, 1491 (1973).
[36]D. Jérome, W. Müller, and M. Weger, J. Phys. Lett. 35, L77 (1974).
[37]W. H. G. Müller and D. Jérome, J. Phys. Lett. 35, L103 (1974).
[38]S. K. Khanna, E. Ehrenfreund, A. F. Garito, and A. J. Heeger, Phys. Rev. B 10, 2205 (1974).
[39]R. H. Blessing and P. Coppens, Solid State Commun. 15, 215 (1974).
[40]A. A. Bright, A. F. Garito, and A. J. Heeger, Phys. Rev. B 10, 1328 (1974).
[41]H. Gutfreund, B. Horovitz, and M. Weger, Solid State Commun. 15, 849 (1974).
[42]R. P. Groff, A. Suna, and R. E. Merrifield, Phys. Rev. Lett. 33, 418 (1974).
[43]M. Weger, B. Horovitz, H. Gutfruend, Phys. Rev. B (to be published).
[44]L. P. Gor'Kov, Zh. Eksp. Teor. Fiz. 65, 1658 (1973) [Sov. Phys.-JETP 38, 830 (1974)].
[45]T. Maniv and M. Weger, J. Phys. Chem. Solids 36, 367 (1975).